NeuroImage: Clinical 36 (2022) 103267

Contents lists available at ScienceDirect

NeuroImage: Clinical

journal homepage: www.elsevier.com/locate/ynicl

Changes in sensory-related brain networks of patients with moyamoya disease with limb paresthesia: A resting-state fMRI-based functional connectivity analysis

Rujing Sun [a,1], Shi-Yu Zhang [a,1], Xu Cheng [a], Peng Zhang [a], Peng-Gang Qiao [a,b,*], Gong-Jie Li [b,*]

[a] Department of Radiology, Beijing Friendship Hospital, Capital Medical University, Beijing, China
[b] Department of Radiology, Affiliated Hospital of Academy of Military Medical Sciences, Beijing, China

ARTICLE INFO

Keywords:
Resting-state functional magnetic resonance imaging
Functional connectivity
Moyamoya disease
Limb paresthesia

ABSTRACT

This study's aim was to investigate functional brain connectivity changes among patients with moyamoya disease (MMD) with limb paresthesia, using functional connectivity analysis based on resting-state functional magnetic resonance imaging (rs-fMRI). A total of 181 patients with MMD were enrolled, including 57 with left limb paresthesia (MLP group), 61 with right limb paresthesia (MRP group), and 63 without paresthesia (MWP group). Encephaloduroarteriosynangiosis (EDAS) was performed in 20 of the 57 patients with left limb paresthesia and 15 of the 61 patients with right limb paresthesia. Twenty-nine age- and sex-matched healthy controls (HC group) were recruited during the same period. All participants underwent rs-fMRI examination, and the patients treated with EDAS were re-examined 3–4 months after the surgery. After data preprocessing, we selected Brodmann area 3 on each side of the brain as the seed region to construct a functional connectivity network of the whole brain, and then we analyzed the differences in functional connectivity between the HC group, MWP group, MLP group, and MRP group. The functional connectivity of Brodmann area 3 (on either side) with the ipsilateral frontal (superior frontal gyrus, middle frontal gyrus, and inferior frontal gyrus) and parietal (supramarginal gyrus, angular gyrus, and superior parietal lobule) cortices was increased among patients with MMD. The functional connectivity enhancement in these brain regions was broader and greater in patients with contralateral limb paresthesia than in patients without paresthesia, and the regions with functional connectivity changes were roughly distributed symmetrically among the MLP group and the MRP group. There were no changes 3–4 months after EDAS in the increased functional connectivity between the frontal and parietal cortices and Brodmann area 3. Limb paresthesia in patients with MMD may be driven by abnormal functional connectivity in the frontal and parietal cortices. Functional changes in associated brain regions may be a target for evaluating the severity of MMD and its response to treatment.

1. Introduction

Moyamoya disease (MMD) is a cerebrovascular disease characterized by the "puff-of-smoke" appearance of abnormal vessel networks at the base of the brain, compensating for chronic occlusion of bilateral internal carotid arteries (Kuroda et al., 2008; Kazumata et al., 2016). The pathophysiology, natural history, and prognostic factors of MMD remain unknown. MMD is manifested by various clinical symptoms, such as myasthenia, sensory disturbances, and disturbances in consciousness, as well as headache and lalopathy. Different clinical symptoms are not associated with specific changes on conventional imageological examinations. Patients with MMD may have different clinical manifestations in long-term chronic ischemic conditions even when their Suzuki stage is identical and conventional MRI sequences detects no changes in brain parenchyma (Hara et al., 2018). In addition, although the clinical symptoms of patients with MMD are closely related to their hemodynamic damage, the two are not positively correlated in all cases. Cases of severe hemodynamic damage may have mild clinical symptoms, or cases

* Corresponding authors at: Department of Radiology, Beijing Friendship Hospital, Capital Medical University, 95 YongAn Road, Beijing 100050, China, (P.-G. Qiao). Department of Radiology, Affiliated hospital of Academy of Military Medical Sciences, #8 Fengtai dong street, Fengtai district, Beijing 100071, China, (G.-J. Li).

E-mail addresses: qiaopenggang@sina.com (P.-G. Qiao), ligj307@sina.com (G.-J. Li).

[1] Equal contribution authors.

https://doi.org/10.1016/j.nicl.2022.103267
Received 19 August 2022; Received in revised form 25 October 2022; Accepted 11 November 2022
Available online 12 November 2022

of mild hemodynamic damage may have severe clinical symptoms. Similarly, a mismatch between hemodynamic improvement and improvement in clinical symptoms may appear after revascularization. These differences can affect a clinician's choice of the timing of surgery and the evaluation of postoperative efficacy (Hervé et al., 2018). The mismatch between hemodynamic damage and clinical symptoms in patients with MMD may be due to the fact that the existing methods of hemodynamic evaluation are not able to accurately assess microcirculatory perfusion damage in the functional areas of the brain or function remodeling areas of the brain.

Neural function remodeling is closely associated with neurological symptoms (Xing et al., 2021; Ma et al., 2017; Okabe et al, 2016; Cohen et al., 2017; Zhao J et al, 2022). Resting-state functional magnetic resonance imaging (rs-fMRI) is an effective method to explore the functional changes in the whole brain using the blood oxygen level-dependent (BOLD) signal (Biswal et al., 1995), and it can reveal associations between neuroanatomy, fluid intelligence, attention, and task-induced brain activity (Kazumata et al., 2017). The BOLD signal essentially corresponds to neuronal activity, which enables rs-fMRI to examine neural function remodeling in patients with cerebrovascular diseases (Lee et al., 2010; Logothetis et al., 2001). Functional connectivity analysis, which maps the spatial pattern of coherent BOLD activity, is used to depict the correlation between different brain regions or networks (Lei et al., 2014; Chen et al., 2020; Kim et al., 2015; Kim et al, 2013). Because it is simple, sensitive, and interpretable, this technique has recently been applied to the study of neurobehavioral dysfunction in stroke patients, as well as vascular cognitive impairments (Siegel et al, 2016; Diciotti et al, 2017). Changes in the resting-state brain network connectivity of patients with MMD have been found to be related to their cognitive performance (Kazumata et al., 2017).

Patients with MMD usually present with a sensory disturbance in the limbs. Studies have revealed that chronic continuous abnormal sensory inputs, such as pain and numbness, may affect the sensory processing of patients (Pei et al., 2020). Currently, there is no study of changes in resting-state brain functional connectivity in patients with MMD with limb paresthesia. Our previous studies that used median nerve electrical stimulation found significant changes in the BOLD-response in the bilateral S1 regions of patients with MMD with unilateral limb paresthesia (Qiao et al., 2017; Qiao et al., 2019), but it is not clear whether patients with MMD with limb paresthesia have any unique characteristics of neural remodeling. Brodmann area 3 (Kim et al., 2015; Kim et al, 2013; Gustin et al., 2012; Kim et al., 2017) is the primary sensory cortex responsible for processing touch sensation, damage to which confers characteristic somatosensory impairment, such as a loss of sensation or reduced sensitivity to sensory stimuli (Kim et al, 2013; Bassett and Sporns, 2017). Including patients with MMD with paresthesia in the limbs in this study made it possible to conduct a rs-fMRI-based functional connectivity analysis by constructing a global functional connectivity network with the Brodmann area 3 on each side of the brain as the seed region. This study aimed to analyze changes in the sensory-related functional network in the brain of patients with MMD to explore the neural remodeling process in the sensory-related functional areas of the brain in patients with MMD with limb paresthesia, and to explore the potential of these alterations as a target for evaluating the severity of the disease and its response to treatment. The ethics committee of *** approved this study.

2. Methods

2.1. Participants

A total of 181 patients with MMD were recruited in this study from January 2015 to July 2018, including 57 with left limb paresthesia (MLP group), 61 with right limb paresthesia (MRP group), and 63 without paresthesia (MWP group). The patients with paresthesia presented with paroxysmal numbness or hypoesthesia of the limbs. Encephaloduroarteriosynangiosis (EDAS) was performed on 20 of the 57 patients with left paresthesia and 15 of the 61 patients with right paresthesia. During the same period, 29 age- and sex-matched healthy controls (HC group) in this study.

The inclusion criteria were: (i) confirmed MMD staged by digital subtraction angiography; (ii) stable disease, no cerebral infarction on conventional MRI or cerebral hemorrhage before scanning, and able to cooperate with examinations; (iii) no additional neurological or psychiatric disorders; and (iv) a right hand preference. All the patients underwent rs-fMRI within one week before or after digital subtraction angiography. The 35 cases undergoing EDAS had another rs-fMRI examination 3–4 months after surgery. All the participants were informed of the details of examinations, and they provided their written consent.

The exclusion criteria were: (i) current or previous neurological and psychiatric diseases (ischemic cerebrovascular disease, diabetes mellitus, peripheral neuropathy, etc.); (ii) unable to tolerate or cooperate with examinations; (iii) organic intracranial lesions on MRI; or (iv) poor image quality due to head motion.

2.2. Physiological and biochemical tests

All the patients completed a set of physiological and biochemical tests before rs-fMRI acquisition to obtain data on systolic pressure, diastolic pressure, blood glucose, total cholesterol, etc. Information on smoking and drinking was also collected.

2.3. MRI data acquisition

Rs-fMRI was performed on all the participants using a Skyra 3 T MRI scanner (Siemens AG, Erlangen, Germany) with a 32-channel standard head coil. Scanning parameters were: echo-planar imaging sequence; repetition time = 2000 ms; echo time = 30 ms; fractional anisotropy = 90°; field of view = 384 mm × 384 mm; number of slices = 33; resolution = 3 mm × 3 mm × 3 mm; and time frame = 6 min and 42 s.

2.4. Data preprocessing

MRI data were preprocessed using the Resting-state fMRI Data Analysis Toolkit (REST, https://www.restfmri.net/) and Statistical Parametric Mapping 12.0 (Wellcome Center for Human Neuroimaging, UCL Queen Square Institute of Neurology). First, we checked the data by naked-eye observation to exclude those of poor quality. Then, we used dcm2nii to convert DICOM data to NII data. The first 10 time points were removed to avoid the potential influence of noise and patient's adaptation period. Slice timing correction was conducted, followed by head motion correction while discarding images with head translation more than 2 mm or rotation more than 2°. A sample-specific diffeomorphic anatomical registration based on the exponentiated Lie algebra template was created using structural images from all the participants. Then, the echo-planar imaging volumes were normalized to MNI space using the diffeomorphic anatomical registration through the exponentiated Lie algebra template and the corresponding flow field. The resampling voxel size was 3 mm × 3 mm × 3 mm. Slice timing, head motion correction, and spatial normalization to the SPM12 Montreal Neurological Institute (MNI) template were performed. The following steps included smoothing (smoothing kernel, 6 × 6 × 6), detrending, regressing out covariates (including head motion and Friston-24 parameters, mean white matter signal, mean cerebrospinal fluid signal, and mean global signal). The Friston 24-parameter model of head motion includes six standard head motion parameters; the derivative of the standard motion parameters is used to account for a one-frame delay in the effect of motion on the BOLD signal, and the 12 corresponding squared items. Additionally, the mean framewise displacement (FD) was calculated, which considers measures of voxelwise differences in motion in its derivation as a measure of the microhead motion of each participant. Linear detrending and a temporal filter (0.01–0.08 Hz) were applied to reduce low-frequency

drifts and high-frequency physiological noise.

2.5. Region of interest-wise functional connectivity analysis

We selected Brodmann area 3 on each side of the brain as the seed region to construct a global functional connectivity network. Calculations were made using REST. For each region of interest (ROI), the seed reference time course was acquired by averaging the time series of all the voxels in the ROI. The mean time course of each ROI was correlated with every other ROI to obtain an n × n matrix of correlation coefficients (r) for every participant. A Fisher r-to-z transformation was applied to improve the normality of the r values.

2.6. Statistical analysis

SPSS 23.0 was used for the statistical analyses. We used one-way analysis of variance to compare the demographic and clinical characteristics of the MWP group, MLP group, and MRP group. The least significant difference *t*-test was used for pairwise comparisons among the three groups when the variances were equal, while Dunnett's T3 was used when the variances were unequal. The chi-square test was used to compare categorical data between groups. For these comparisons, $P < 0.05$ was considered to be statistically significant. The two-sample *t*-test was performed to compare functional connectivity between the HC group, MWP group, MLP group, and MRP group. $q < 0.05$ (after adjusting for the false discovery rate) was considered to be statistically significant.

3. Results

3.1. Demographic data

There were no significant differences in sex, age, diabetes, hypertension, hyperlipidemia, or a history of smoking or drinking between the MWP group, MLP group, and MRP group (Table 1). (See Tables 3 and 4).

3.2. Overview of motion in the data

Two subjects with motion greater than 2 mm or 2 degrees of rotation were excluded (including one subject from MWP, one from MRP). Table 2 shows the quantification of the movement parameter (measures of mean framewise displacement) of the four groups. The results show there were no significant differences in the movement parameters between the four groups.

3.3. Functional connectivity comparisons between groups

Using Brodmann area 3 on either side as the seed region to construct a functional connectivity network of the whole brain, compared with the healthy controls, the patients with MMD had some brain regions with increased functional connectivity and some regions with decreased

Table 1
Demographic data of the study subjects.

	MRP(n = 61)	MLP(n = 57)	MWP(n = 63)	F	P
Age, years, mean ± SD	37.6 ± 10.7	36.7 ± 9.9	40.4 ± 9.79	2.232	0.110
Gender Male, n(%)	34(55.7)	28(49.1)	28(44.4)	0.790	0.455
Female, n(%)	27(44.3)	29(50.9)	35(55.6)		
Diabetes, n(%)	2(3.3)	6(10.5)	3(4.8)	1.502	0.225
Hypertension, n(%)	26(42.6)	15(26.3)	21(33.3)	1.763	0.175
Hyperlipidemia, n (%)	6(9.8)	5(8.8)	12(19.0)	1.771	0.173
Smoking, n(%)	17(27.9)	11(19.3)	16(25.4)	0.613	0.543
Drinking, n(%)	11(18.0)	9(15.8)	18(28.6)	1.721	0.182

Table 2
Overview of motion in the data.

	HC(n = 29)	MWP(n = 62)	MLP(n = 57)	MRP(n = 60)	F	P
Mean framewise displacement	0.11 ± 0.36	0.11 ± 0.04	0.11 ± 0.04	0.12 ± 0.04	1.293	0.278

Data presented as mean ± SD. One-way ANOVA, SPSS 23.

Table 3
Brain regions showing decreased and increased effective connectivity from the left Brodmann area 3.

Region	MNI coordinates			Size (voxels)	Peak *T*-value
	x	y	z		
MLP > HC					
Decreased					
Calcarine_L	27	−57	3	957	−4.8854
Temporal_Inf_R	45	−60	−3	160	−5.776
Postcentral_R	42	−21	36	2756	−6.2181
Increased					
Frontal_Mid_L	−39	51	15	332	5.0598
Frontal_Mid_L	−39	0	51	746	5.6917
Parietal_Inf_L	−39	−54	45	341	4.0934
Precuneus_R	0	−57	66	135	5.9013
MLP > MWP					
Decreased					
Occipital_Mid_L	−21	−84	0	129	−3.506
Frontal_Mid_R	48	48	21	75	−4.0058
Frontal_Sup_R	15	6	54	73	−3.946
Increased					
Putamen_L	–33	−9	0	52	4.3307
Postcentral_L	−30	−42	54	72	3.9527
MWP > HC					
Decreased					
Calcarine_R	21	−69	15	401	−4.5608
ParaHippocampal_R	21	−12	−21	52	−4.7215
Lingual_L	−15	−45	−6	153	−4.1615
Hippocampus_L	−12	−24	0	61	−4.5524
Temporal_Inf_R	45	−60	−3	141	−5.1138
Lingual_R	6	−69	0	50	−4.0392
Postcentral_R	42	−24	18	2427	−6.0595
Increased					
Frontal_Mid_L	−21	54	33	164	3.8293
SupraMarginal_L	−63	−39	18	182	4.6291
Precentral_L	−42	0	54	597	5.9251
Frontal_Sup_R	18	18	48	137	3.9668
MRP > HC					
Decreased					
Postcentral_R	54	−18	42	7971	−7.0461
Hippocampus_L	−30	−15	−27	85	−4.236
Occipital_Inf_L	−42	−63	−6	96	−3.8122
Increased					
Cerebelum_Crus1_R	−3	−87	−39	588	4.9369
Frontal_Mid_L	−42	3	51	2726	8.1379
Parietal_Inf_L	−42	−39	33	1505	5.9089
Caudate_L	−15	−12	24	110	5.0663
Parietal_Inf_R	60	−60	42	153	4.2373
Frontal_Mid_R	48	24	48	89	3.6849
MRP > MWP					
Decreased					
Frontal_Inf_Orb_R	24	39	−9	69	−3.904
Frontal_Mid_R	30	39	15	52	−4.1849
Increased					
Cerebelum_Crus2_R	48	−60	−42	127	4.3662
Frontal_Mid_L	−51	24	12	481	4.3504
Parietal_Inf_L	−45	−42	51	529	4.4224

MNI, Montreal Neurological Institute.

Table 4
Brain regions showing decreased and increased effective connectivity from the right Brodmann area 3.

Region	MNI coordinates			Size (voxels)	Peak *T*-value
	x	y	z		
MLP > HC					
Decreased					
Cerebelum_8_L	−9	−69	−45	58	−4.143
ParaHippocampal_L	−21	−6	−24	67	−3.5416
Postcentral_L	45	−54	−9	10,143	−7.7765
ParaHippocampal_R	18	−12	−21	54	−4.3319
Thalamus_R	15	−24	0	252	−7.4466
Increased					
Cerebelum_9_L	6	−45	−48	202	4.4306
Temporal_Inf_L	−66	−21	−18	386	5.0615
Cerebelum_Crus1_R	6	−90	−30	1366	5.9227
Temporal_Inf_R	63	−18	−33	219	4.1791
Frontal_Mid_R	42	6	54	4049	8.6136
Frontal_Inf_Orb_L	−45	36	−18	101	4.3397
Caudate_R	15	3	21	276	6.7295
Frontal_Mid_L	–33	63	6	79	3.601
Angular_L	−48	−63	51	595	4.8362
Angular_R	51	−51	39	1048	5.5833
Precuneus_L	−9	−54	36	84	3.1877
Precuneus_R	6	−48	75	123	5.1866
MLP > MWP					
Decreased					
Occipital_Mid_L	−45	−69	12	81	−4.6745
Parietal_Sup_L	−18	−54	51	74	−4.1646
Increased					
Cerebelum_Crus1_R	30	−66	−39	88	4.6779
Cerebelum_Crus1_L	−45	−75	−39	66	4.8338
Frontal_Sup_R	39	45	−15	420	4.7766
Cingulum_Ant_R	9	39	15	61	3.9362
Precuneus_L	−6	−60	24	195	4.2578
Angular_L	–33	−63	39	56	3.9487
Frontal_Mid_R	42	12	51	261	4.275
MWP > HC					
Decreased					
Lingual_R	21	−42	−12	543	−5.1213
Lingual_L	−39	−57	−9	1097	−5.3382
Postcentral_L	–33	−12	0	2155	−7.1066
Thalamus_R	15	−24	−3	133	−5.7232
Increased					
Cerebelum_Crus2_R	6	−87	–33	163	4.4188
Cerebelum_Crus1_L	−54	−57	−36	55	4.3309
Frontal_Inf_Orb_L	−54	24	−6	51	3.8039
Frontal_Mid_Orb_R	42	60	−6	119	4.6538
Frontal_Inf_Tri_R	54	18	0	90	4.1505
Angular_R	69	−51	15	575	5.2337
Caudate_R	18	3	24	106	4.462
Frontal_Mid_R	48	21	33	1284	5.5289
Frontal_Sup_Medial_R	0	39	48	59	4.0096
Precuneus_R	6	−63	69	94	4.2273
MRP > HC					
Decreased					
Lingual_R	45	−54	−9	4929	−5.3653
Postcentral_L	−45	−24	66	3427	−7.2762
Increased					
Cerebelum_Crus1_L	−48	−78	−30	68	3.983
Cerebelum_Crus2_R	21	−87	–33	254	4.3392
Temporal_Mid_L	−66	−21	−18	85	4.486
Frontal_Mid_Orb_R	39	63	−9	131	3.7003
Caudate_R	18	9	18	163	5.3418
Angular_R	45	−36	33	1088	4.2567
Angular_L	−48	−63	51	419	4.5429
Frontal_Mid_R	42	6	54	2715	6.2233
Precuneus_R	3	−57	66	165	4.9727
MRP > MWP					
Increased					
Postcentral_R	30	−39	45	169	4.1229
Frontal_Sup_R	30	−12	48	71	3.9913
Frontal_Sup_Medial_R	12	33	45	51	4.0337

MNI, Montreal Neurological Institute.

functional connectivity (Fig. 1-Fig. 3). The detail areas for the FC results together with the statistical values and coordinates are summarized in Supplementary Tab. 3 and Tab. 4. Since patients with MMD suffer from long-term ischemia in brain tissue, the reduction in functional connectivity is probably associated with hemodynamic changes. In this context, functional connectivity enhancement is deemed to be more powerful to detect changes in the neural activity of associated functional areas. Thus, we mainly focused on the brain regions with increased functional connectivity.

Using the left Brodmann area 3 as the seed region to construct the global functional connectivity network, compared to the HC group, the MWP group had increased functional connectivity in the superior frontal gyrus, middle frontal gyrus, inferior frontal gyrus, supramarginal gyrus, and angular gyrus on the left side and the superior frontal gyrus and middle frontal gyrus on the right side (Fig. 1A); the MRP group had increased functional connectivity in the superior frontal gyrus, middle frontal gyrus, inferior frontal gyrus, angular gyrus, supramarginal gyrus, and superior parietal gyrus on the left side, and the superior frontal gyrus, middle frontal gyrus, supramarginal gyrus, and angular gyrus on the right side (Fig. 2A); the MLP group had increased functional connectivity in the middle frontal gyrus, superior frontal gyrus, inferior frontal gyrus, supramarginal gyrus, and angular gyrus on the left side (Fig. 3A). Compared to the MWP group, the MRP group had increased functional connectivity in the middle frontal gyrus, inferior frontal gyrus, supramarginal gyrus, angular gyrus, and superior parietal gyrus on the left side (Fig. 2C). In contrast, the MLP group had increased functional connectivity in the left superior parietal gyrus and angular gyrus compared to the MWP group (Fig. 3C).

Using the right Brodmann area 3 as the seed region to construct the global functional connectivity network, compared to the HC group, the MWP group had increased functional connectivity in the left inferior frontal gyrus and the right middle frontal gyrus, superior frontal gyrus, inferior frontal gyrus, supramarginal gyrus, angular gyrus, and superior parietal gyrus among the patients with MMD without paresthesia (Fig. 1B); the MLP group had increased functional connectivity in the middle frontal gyrus, superior frontal gyrus, inferior frontal gyrus, angular gyrus, and superior parietal gyrus on the right side, and the middle frontal gyrus, superior frontal gyrus, angular gyrus, supramarginal gyrus, and superior parietal gyrus (Fig. 2B); the MRP group had increased functional connectivity in the angular gyrus and superior parietal gyrus on the left side and the middle frontal gyrus, superior frontal gyrus, inferior frontal gyrus, angular gyrus, and superior parietal gyrus on the right side among those with right limb paresthesia (Fig. 3B). Compared to the MWP group, the MLP group had increased functional connectivity in the superior frontal gyrus, middle frontal gyrus, and inferior frontal gyrus on the right side and the angular gyrus and superior parietal gyrus on the left side (Fig. 2D). In contrast, the MRP group had increased functional connectivity in the superior frontal gyrus, middle frontal gyrus, supramarginal gyrus, angular gyrus, and superior parietal gyrus on the right side (Fig. 3D).

The regions with functional connectivity changes were roughly distributed symmetrically among patients with left limb paresthesia and those with right limb paresthesia.

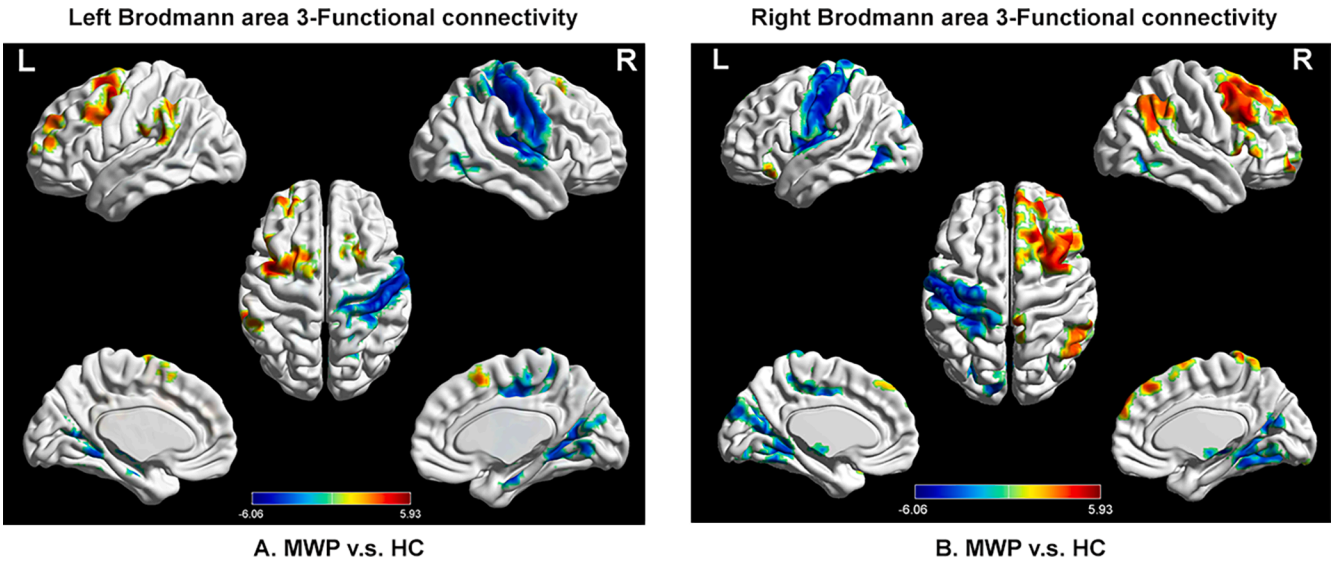

Fig. 1. This figure compares the functional connectivity changes of the healthy controls (HC) to those of MMD patients without paresthesia (MWP), using the left Brodmann area 3 (Fig. 1A) and the right Brodmann area 3 (Fig. 1B) as the seed region to construct the global functional connectivity network.

3.4. Functional connectivity changes after EDAS in patients with MMD with unilateral limb paresthesia

Among the 20 cases of MMD with left limb paresthesia who underwent right EDAS, the limb symptoms disappeared in 12 cases and lessened in 8 cases 3–4 months after the operation. There were no significant changes after the operation in functional connectivity between brain regions and the seed region Brodmann area 3 on either side.

Among the 15 cases of MMD with right limb paresthesia who underwent left EDAS, the limb symptoms disappeared in 9 cases and lessened in 6 cases 3–4 months after the operation. There were no significant changes in functional connectivity after the operation between brain regions and the seed region Brodmann area 3 on either side.

4. Discussion

This study detected changes in sensory-related functional connectivity in the brain among patients with MMD using rs-fMRI-based functional connectivity analysis. We found that patients with MMD with limb paresthesia differed in sensory-related functional connectivity from patients with MMD without limb paresthesia and healthy subjects. Moreover, the regions with functional connectivity changes were, in general, symmetrically distributed among those with left limb paresthesia and those with right limb paresthesia. The results can be verified mutually and are convincing.

4.1. The frontal and parietal cortices are the key brain regions involved in the neural remodeling process in patients with MMD with limb paresthesia

Functional reorganization of the somatosensory system has been observed after brain lesion or bodily injury (Lemée et al., 2020; Zhao et al., 2016). Our results showed decreased functional connectivity between the seed region Brodmann area 3 and the contralateral Brodmann area 3, and increased functional connectivity between the seed region Brodmann area 3 on either side and the frontal (superior frontal gyrus, middle frontal gyrus, and inferior frontal gyrus) and parietal (supramarginal gyrus, angular gyrus, and superior parietal lobule) cortices on the ipsilateral side in patients with MMD without limb paresthesia. It suggested that patients with MMD have decreased functional connectivity between Brodmann area 3 and the contralateral Brodmann area 3 due to long-term chronic ischemia and they also have increased functional connectivity between Brodmann area 3 and the frontal and parietal cortices on the ipsilateral side even in patients without limb paresthesia. However, the functional connectivity enhancement in these regions was broader and greater among patients with contralateral limb paresthesia, compared with patients without limb paresthesia, and functional connectivity with the contralateral frontal cortex was enhanced. These results revealed the possible neural remodeling process related to Brodmann area 3 in patients who have MMD with limb paresthesia; that is, the functional connectivity with the ipsilateral frontal and parietal cortices was from weak to strong in strength and from small to broad in range. In the process, the frontal and parietal cortices were the key brain regions. It has been demonstrated that the prefrontal cortex is a key node in the executive control network; the dorsolateral prefrontal cortex has been deemed to be the core area for pain processing, with extensive links to both sensory and motor cortices (Pei et al., 2020; Kong et al., 2013; Craig, 2003; Willis et al., 2002; Bushnell et al., 1999). Our findings suggest a close association of functional changes in the prefrontal cortex with the sensory disturbances in the limbs of patients with MMD. Of the parietal cortices with increased functional connectivity, the angular gyrus/supramarginal gyrus (AG/SG) is the core of the default mode network (Su et al., 2016; Hagmann et al., 2008). Located at the junction between the temporal, parietal, and occipital lobes, the AG/SG is considered to be the main hub connecting different subsystems that play key roles in various cognitive and behavioral processes (Seghier, 2013). Studies on the association of the AG/SG with limb paresthesia have not yet been reported. In this study, patients with MMD with unilateral limb paresthesia showed increased functional connectivity between the contralateral Brodmann area 3 and the AG/SG, indicating that the AG/SG may be an important brain region involved in sensory abnormalities of the limbs. Therefore, functional changes in the frontal (superior frontal gyrus, middle frontal gyrus, and inferior frontal gyrus) and parietal (supramarginal gyrus, angular gyrus, and superior parietal lobule) cortices may be targets for disease evaluation and follow-up for patients with MMD and serve as new neural bases for the diagnosis and treatment of this disease.

4.2. A broader range of neural remodeling was observed in patients with MMD with right limb paresthesia versus those with left limb paresthesia

We also found when we used the Brodmann area 3 contralateral to symptoms as the seed region, that patients with MMD with right limb paresthesia showed a broader and greater increase in functional connectivity compared with those with left limb paresthesia. This may be

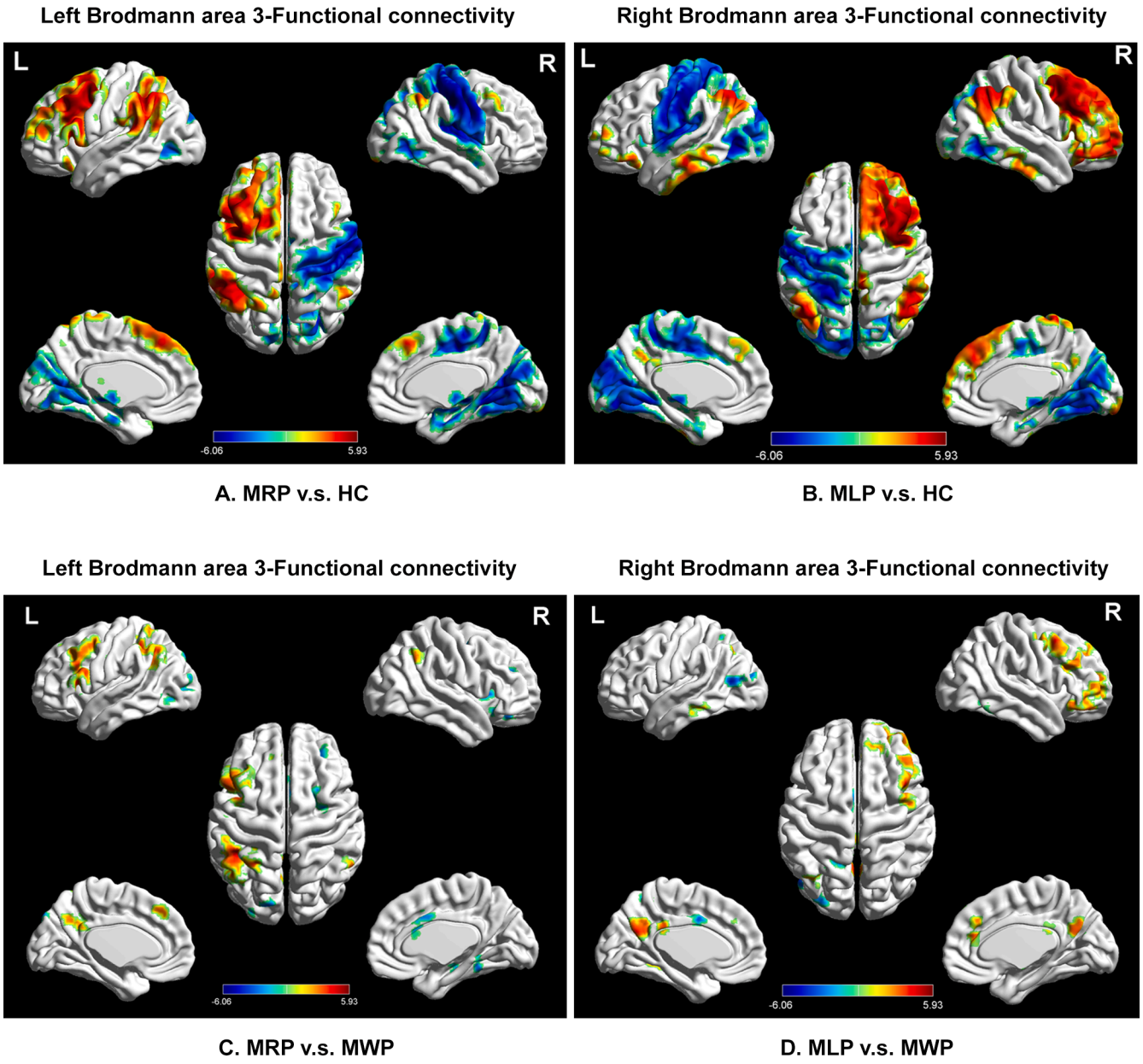

Fig. 2. This figure compares the the functional connectivity changes of healthy controls (HC) to those of MMD patients without paresthesia (MWP) and MMD patients with right limb paresthesia (MRP), using the left Brodmann area 3 as the seed region (Fig. 2A,C), and those of MMD patients with left limb paresthesia (MLP), using the right Brodmann area 3 as the seed region to construct the global functional connectivity network (Fig. 2B,D).

due to the right hand preference of our participants. On the one hand, right-handed patients are more sensitive to subtle changes in the sensation of the right limbs, so even mild damage can affect or remodel neural activity in associated brain regions. On the other hand, the somatosensory networks are lateralized. Right-handed patients have been found to have stronger between-hemispheres connectivity, and left-handed patients have stronger within-hemisphere connectivity. In addition, the regions showing greater connectivity were the posterior regions of the brain in left-handed patients and the frontal regions in right-handed patients (Tejavibulya et al., 2022). The difference in functional connectivity between patients with MMD with right hand paresthesia and those with left hand paresthesia may also be related to the lateralization of somatosensory networks.

However, there were no changes 3–4 months after revascularization in the functional connectivity between the frontal and parietal cortices and Brodmann area 3 among the patients with MMD with limb paresthesia who underwent EDAS, although their clinical symptoms had resolved. This suggests that the functional remodeling of the frontal and parietal cortices of these patients may persist for a long time after the operation, which needs further study to examine its clinical value.

4.3. Limations

This study has some limitations. First, we only focused on functional connectivity changes in the brain regions associated with Brodmann area 3, and we did not obtain information on the connections between different brain networks, such as the default mode network. However, the interaction between different networks may provide more clues about the central mechanism of limb paresthesia in patients with MMD. Second, patients were only re-examined 3–4 months after surgery; hence the study lacks long-term follow-up data that can help better reveal functional connectivity changes with the improvement of cerebral hemodynamics. Third, we only analyzed functional connectivity changes of the whole brain with Brodmann area 3 as the seed region in patients

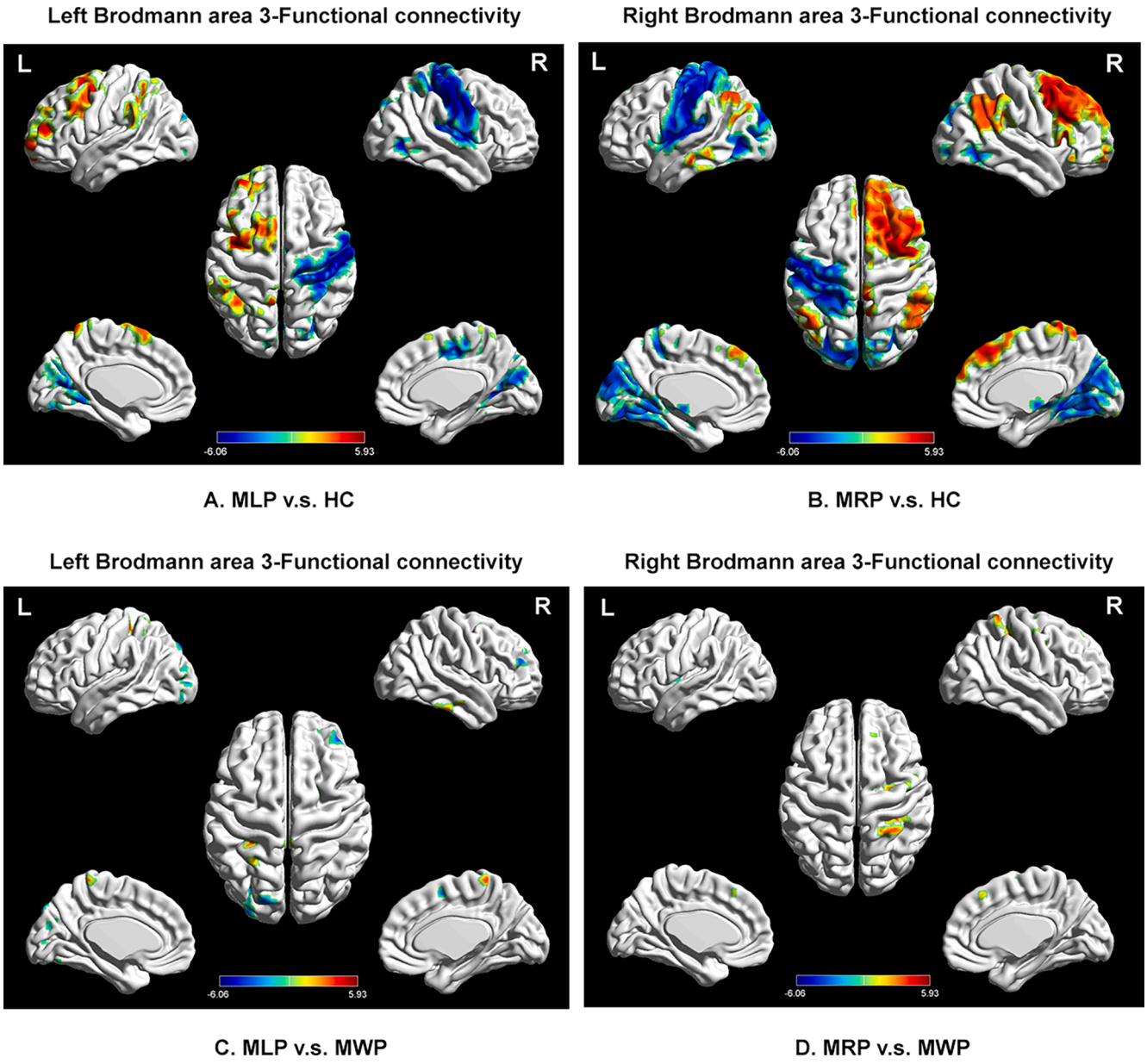

Fig. 3. This figure compares the functional connectivity changes of the healthy controls (HC) to those of MMD patients without paresthesia (MWP) and MMD patients with left limb paresthesia (MLP), using the left Brodmann area 3 as the seed region (Fig. 3A,C), and those of MMD patients with right limb paresthesia (MRP) using the right Brodmann area 3 as the seed region to construct the global functional connectivity network (Fig. 3B,D).

with MMD with limb paresthesia, which was not sufficient to comprehensively reflect the changes in sensory-related functional networks in patients with MMD.

5. Conclusion

This rs-fMRI-based functional connectivity analysis revealed increased functional connectivity between Brodmann area 3 and the frontal (superior frontal gyrus, middle frontal gyrus, and inferior frontal gyrus) and parietal (supramarginal gyrus, angular gyrus, and superior parietal lobule) cortices among patients with MMD with limb paresthesia. Therefore, limb paresthesia may be a result of abnormal functional activity in those associated cortices. Functional changes in associated brain regions may be a target for evaluating the severity of MMD and its response to treatment.

6. Grant support

This work was supported by grants from National Natural Science Foundation of China (No.81701663), Beijing Hospitals Authority Clinical Medicine Development of Special Funding Support (ZYLX202101), and Beijing Municipal Health Commission, Beijing key Clinical Discipline Funding (Grant No 2021-135).

CRediT authorship contribution statement

Rujing Sun: Conceptualization, Methodology, Data curation, Formal analysis, Writing – original draft, Writing – review & editing. **Shi-YuZhang:** Conceptualization, Methodology, Writing – review & editing. **Xu Cheng:** Data curation. **Peng Zhang:** Data curation. **Peng-Gang Qiao:** Writing – review & editing, Supervision, Funding acquisition. **Gong-Jie Li:** Writing – review & editing, Supervision.

Declaration of Competing Interest

The authors declare that they have no known competing financial interests or personal relationships that could have appeared to influence the work reported in this paper.

Data availability

Data will be made available on request.

Acknowledgements

This work was supported by grants from National Natural Science Foundation of China (No.81701663), Beijing Hospitals Authority Clinical Medicine Development of Special Funding Support (ZYLX202101), and Beijing Municipal Health Commission, Beijing key Clinical Discipline Funding (grant number 2021-135).

References

Bassett, D.S., Sporns, O., 2017. Network neuroscience. Nat. Neurosci. 20, 353–364. https://doi.org/10.1038/nn.4502.

Biswal, B., Yetkin, F.Z., Haughton, V.M., Hyde, J.S., 1995. Functional connectivity in the motor cortex of resting human brain using echo-planar mri. Magn. Resonance Med.. 34, 537–541. https://doi.org/10.1002/mrm.1910340409.

Bushnell, M.C., Duncan, G.H., Hofbauer, R.K., Ha, B., Chen, J.-I., Carrier, B., 1999. Carrier B. Pain perception: is there a role for primary somatosensory cortex? Proc. Natl. Acad. Sci. USA 96 (14), 7705–7709.

Chen, Z., Zhao, R., Wang, Q., Yu, C., Li, F., Liang, M., Zong, Y., Zhao, Y., Xiong, W., Su, Z., Xue, Y., 2020. Functional Connectivity Changes of the Visual Cortex in the Cervical Spondylotic Myelopathy Patients: A Resting-State fMRI Study. Spine 45, E272–E279. https://doi.org/10.1097/BRS.0000000000003245.

Cohen, E.J., Quarta, E., Bravi, R., Granato, A., Minciacchi, D., 2017. Neural plasticity and network remodeling: From concepts to pathology. Neuroscience 344, 326–345. https://doi.org/10.1016/j.neuroscience.2016.12.048.

Craig, A.D.B., 2003. Pain mechanisms: labeled lines versus convergence in central processing. Annu. Rev. Neurosci. 26, 1–30. https://doi.org/10.1146/annurev.neuro.26.041002.131022.

Diciotti, S., Orsolini, S., Salvadori, E., Giorgio, A., Toschi, N., Ciulli, S., Ginestroni, A., Poggesi, A., De Stefano, N., Pantoni, L., Inzitari, D., Mascalchi, M., VMCI Tuscany investigators, 2017. Resting state fMRI regional homogeneity correlates with cognition measures in subcortical vascular cognitive impairment. J. Neurol. Sci. 373, 1–6. https://doi.org/10.1016/j.jns.2016.12.003.

Gustin, S.M., Peck, C.C., Cheney, L.B., Macey, P.M., Murray, G.M., Henderson, L.A., 2012. Pain and plasticity: is chronic pain always associated with somatosensory cortex activity and reorganization? J. Neurosci. 32, 14874–14884. https://doi.org/10.1523/JNEUROSCI.1733-12.2012.

Hagmann, P., Cammoun, L., Gigandet, X., Meuli, R., Honey, C.J., Wedeen, V.J., Sporns, O., Friston, K.J., 2008. Mapping the structural core of human cerebral cortex. PLoS Biol. 6 (7), e159.

Hervé, D., Kossorotoff, M., Bresson, D., Blauwblomme, T., Carneiro, M., Touze, E., Proust, F., Desguerre, I., Alamowitch, S., Bleton, J.P., Borsali, A., Brissaud, E., Brunelle, F., Calviere, L., Chevignard, M., Geffroy-Greco, G., Faesch, S., Habert, M. O., De Larocque, H., Meyer, P., Reyes, S., Thines, L., Tournier-Lasserve, E., Chabriat, H., 2018. French clinical practice guidelines for Moyamoya angiopathy. Rev Neurol (Paris). 174, 292–303. https://doi.org/10.1016/j.neurol.2017.12.002.

Kazumata, K., Tha, K.K., Narita, H., Ito, Y.M., Shichinohe, H., Ito, M., Uchino, H., Abumiya, T., 2016. Characteristics of diffusional kurtosis in chronic ischemia of adult moyamoya disease: comparing diffusional kurtosis and diffusion tensor imaging. AJNR Am. J. Neuroradiol. 37, 1432–2149. https://doi.org/10.3174/ajnr.a4728.

Kazumata, K., Tha, K.K., Uchino, H., Ito, M., Nakayama, N., Abumiya, T., Hayasaka, S., 2017. Mapping altered brain connectivity and its clinical associations in adult moyamoya disease: A resting-state functional MRI study. PLoS One 12 (8). https://doi.org/10.1371/journal.pone.0182759.

Kim, W., Kim, S.K., Nabekura, J., 2017. Functional and structural plasticity in the primary somatosensory cortex associated with chronic pain. J. Neurochem. 141, 499–506. https://doi.org/10.1111/jnc.14012.

Kim, J., Loggia, M.L., Edwards, R.R., Wasan, A.D., Gollub, R.L., Napadow, V., 2013. Sustained deep-tissue pain alters functional brain connectivity. Pain 154, 1343–1351. https://doi.org/10.1016/j.pain.2013.04.016.

Kim, J., Loggia, M.L., Cahalan, C.M., Harris, R.E., Beissner, F., Garcia, R.G., Kim, H., Barbieri, R., Wasan, A.D., Edwards, R.R., Napadow, V., 2015. The somatosensory link in fibromyalgia: functional connectivity of the primary somatosensory cortex is altered by sustained pain and is associated with clinical/autonomic dysfunction. Arthritis Rheumatol. 67 (5), 1395–1405.

Kong, J., Spaeth, B., Wey, H., Cheetham, A., Cook, A.H., Jensen, K., Tan, Y., Liu, H., Wang, D., Loggia, M.L., Napadow, V., Smoller, J.W., Wasan, A.D., Gollub, R.L., 2013. S1 is associated with chronic low back pain: a functional and structural MRI study. Mol Pain. 9, 43. https://doi.org/10.1186/1744-8069-9-43.

Kuroda, S., Houkin, K., 2008. Moyamoya disease: current concepts and future perspectives. Lancet Neurol. 7, 1056–1066. https://doi.org/10.1016/S1474-4422(08)70240-0.

Lee, J.H., Durand, R., Gradinaru, V., Zhang, F., Goshen, I., Kim, D.S., Fenno, L.E., Ramakrishnan, C., Deisseroth, K., 2010. Global and local fMRI signals driven by neurons defined optogenetically by type and wiring. Nature 465, 788–792. https://doi.org/10.1038/nature09108.

Lei, Y., Li, Y., Ni, W., Jiang, H., Yang, Z., Guo, Q., Gu, Y., Mao, Y., 2014. Spontaneous brain activity in adult patients with moyamoya disease: a resting-state fMRI study. Brain Res. 1546, 27–33. https://doi.org/10.1016/j.brainres.2013.12.022.

Lemée, J.M., Chinier, E., Ali, P., Labriffe, M., Ter Minassian, A., Dinomais, M., 2020. (Re) organisation of the somatosensory system after early brain lesion: A lateralization index fMRI study. Ann Phys Rehabil Med. 63, 416–421. https://doi.org/10.1016/j.rehab.2019.02.001.

Logothetis, N.K., Pauls, J., Augath, M., Trinath, T., Oeltermann, A., 2001. Neurophysiological investigation of the basis of the fMRI signal. Nature 412 (6843), 150–157.

Ma, H., Lu, Y., Hua, X., Shen, Y., Zheng, M., Xu, W., 2017. A Longitudinal fMRI Research on Neural Plasticity and Sensory Outcome of Carpal Tunnel Syndrome. Neural Plasticity. 2017, 5101925. https://doi.org/10.1155/2017/5101925.

Okabe, N., Shiromoto, T., Himi, N., Lu, F., Maruyama-Nakamura, E., Narita, K., Iwachidou, N., Yagita, Y., Miyamoto, O., 2016. Neural network remodeling underlying motor map reorganization induced by rehabilitative training after ischemic stroke. Neuroscience 339, 338–362. https://doi.org/10.1016/j.neuroscience.2016.10.008.

Pei, Y., Zhang, Y., Zhu, Y., Zhao, Y., Zhou, F., Huang, M., Wu, L., Gong, H., 2020. Hyperconnectivity and High Temporal Variability of the Primary Somatosensory Cortex in Low-Back-Related Leg Pain: An fMRI Study of Static and Dynamic Functional Connectivity. J. Pain Res. 13, 1665–2167. https://doi.org/10.2147/JPR.S242807.

Qiao, P.G., Han, C., Qian, T., Li, G.J., Yin, H., 2017. BOLD-fMRI with median nerve electrical stimulation predict hemodynamic improvement after revascularization in patients with moyamoya disease. J. Magn. Reson. Imaging 46, 1159–1166. https://doi.org/10.1002/jmri.25598.

Qiao, P.G., Cheng, X., Zuo, Z.W., Han, C., Yang, Z.H., Li, G.J., 2019. Blood Oxygen Level-Dependent Response Changes in the Ipsilateral Primary Somatosensory Cortex and Thalamus of Patients With Moyamoya Disease During Median Nerve Electrical Stimulation. J. Comput. Assist. Tomogr. 43, 539–546. https://doi.org/10.1097/RCT.0000000000000891.

Seghier, M.L., 2013. The angular gyrus: multiple functions and multiple subdivisions. The Neuroscientist. 19, 43–61. https://doi.org/10.1177/1073858412440596.

Siegel, J.S., Ramsey, L.E., Snyder, A.Z., Metcalf, N.V., Chacko, R.V., Weinberger, K., Baldassarre, A., Hacker, C.D., Shulman, G.L., Corbetta, M., 2016. Disruptions of network connectivity predict impairment in multiple behavioral domains after stroke. Proc Natl Acad Sci U S A. 113, E4367–E4376. https://doi.org/10.1073/pnas.1521083113.

Su, Q., Yao, D., Jiang, M., Liu, F., Long, L., Dai, Y., Yu, M., Zhang, Z., Zhang, J., Liu, J., Xiao, C., Zhao, J., Guo, W., 2016. Decreased interhemispheric functional connectivity in insula and angular gyrus/supramarginal gyrus: Significant findings in first-episode, drug-naive somatization disorder. Psychiatry Res. 248, 48–54. https://doi.org/10.1016/j.pscychresns.2016.01.008.

Tejavibulya, L., Peterson, H., Greene, A., Gao, S., Rolison, M., Noble, S., Scheinost, D., 2022. Large-scale differences in functional organization of left- and right-handed individuals using whole-brain, data-driven analysis of connectivity. Neuroimage. 252, 119040 https://doi.org/10.1016/j.neuroimage.2022.119040.

Willis, W.D., Zhang, X., Honda, C.N., Giesler, G.J., 2002. A critical review of the role of the proposed VMpo nucleus in pain. J. Pain 3 (2), 79–94.

Xing, X.X., Hua, X.Y., Zheng, M.X., Wu, J.J., Huo, B.B., Ma, J., Ma, Z.Z., Li, S.S., Xu, J.G., 2021. Abnormal Brain Connectivity in Carpal Tunnel Syndrome Assessed by Graph Theory. Journal of Pain Research. 4, 693–701. https://doi.org/10.2147/JPR.S289165.

Zhao, J., Guo, X., Xia, X., Peng, W., Wang, W., Li, S., Zhang, Y., Hu, L., 2016. Functional Reorganization of the Primary Somatosensory Cortex of a Phantom Limb Pain Patient. Pain Physician. 19, E781–E786. PMID: 27389122.

Zhao, J., Long, Z., Li, Y., Qin, Y., Liu, Y., 2022. Alteration of regional heterogeneity and functional connectivity for obese undergraduates: evidence from resting-state fMRI. Brain Imaging Behav. 16, 627–636. https://doi.org/10.1007/s11682-021-00542-4.